Counterfactual distributed controlled-phase gate for quantum-dot spin qubits in double-sided optical microcavities

Qi Guo,[1] Liu-Yong Cheng,[1] Li Chen,[1] Hong-Fu Wang,[2] and Shou Zhang[1,2,*]

[1]*Department of Physics, Harbin Institute of Technology, Harbin, Heilongjiang 150001, People's Republic of China*

[2]*Department of Physics, College of Science, Yanbian University, Yanji, Jilin 133002, People's Republic of China*

(Received 19 May 2014; published 22 October 2014)

The existing distributed quantum gates required physical particles to be transmitted between two distant nodes in the quantum network. We here demonstrate the possibility to implement distributed quantum computation without transmitting any particles. We propose a scheme for a distributed controlled-phase gate between two distant quantum-dot electron-spin qubits in optical microcavities. The two quantum-dot-microcavity systems are linked by a nested Michelson-type interferometer. A single photon acting as ancillary resource is sent in the interferometer to complete the distributed controlled-phase gate, but it never enters the transmission channel between the two nodes. Moreover, we numerically analyze the effect of experimental imperfections and show that the present scheme can be implemented with high fidelity in the ideal asymptotic limit. The scheme provides further evidence of quantum counterfactuality and opens promising possibilities for distributed quantum computation.

DOI: 10.1103/PhysRevA.90.042327 PACS number(s): 03.67.Hk, 03.65.−w, 78.67.Hc

I. INTRODUCTION

Counterfactual quantum information processing suggests that relevant quantum information tasks can be achieved without exchanging physical particles between two distant parties, so it has been attracting more and more attention in recent years. Counterfactual quantum communication can be seen as the generalization of interaction-free measurements, which was proposed by Elitzur and Vaidman in 1993 [1] and improved by Kwiat *et al.* in 1995 [2]. The basic idea of these protocols is that if there is an obstructing object in one of the arms of the Mach-Zehnder interferometer, the interference of the photon passing through the interferometer will be destroyed even though the photon was not absorbed by the object at all. Hence the existence or absence of the obstructing object can be revealed by the path information of the photon without interaction between the photon and the object. Subsequently, Hosten *et al.* [3] proposed a counterfactual scheme for implementing Grover's search algorithm by using the "chained" version of the quantum Zeno effect in 2006, which opened the probability for counterfactual quantum computation. Counterfactual quantum key distribution (CQKD) has also been investigated extensively since the first CQKD scheme was presented by Noh in 2009 [4]. Experimentally, CQKD with no particle transmitted has been realized by different research groups [5,6], and its unconditional security was proved in an ideal situation [7,8]. Recently, Salih *et al.* [9] demonstrated that classical information can be transferred from the sender to the receiver without any particles traveling between them, which challenged the long-standing assumption that information transfer requires physical particles to travel between sender and receiver, and attracted much subsequent attention [10–12].

Quantum computation is a central part of quantum information science due to the incredible computational power over its classical counterpart. The building blocks of quantum computation are quantum logic gates. Universal quantum computation can be implemented by single-qubit gates and a two-qubit controlled-NOT gate or a controlled-phase (CPHASE) gate [13], that is, any complex gates can be decomposed into these two elementary logic gates in principle. For a large-scale quantum computation network, it is necessary to perform computational tasks between qubits of distant nodes, which is called distributed quantum computation [14,15]. Many schemes for distributed quantum computation have been put forward in the past few years [16–21]. Undoubtedly, the distributed controlled-NOT or CPHASE gate was the most important part in these schemes. One method to realize the nonlocal interaction was that remote qubits interacted respectively with one particle of a two-body entangled pair, which means prior entanglement sharing is required. Another method was that a mediating particle was transmitted in the quantum channel between the two nodes and interacted with the two separate qubits successively. We also note that some quantum zeno style gates based on interaction-free measurement have been proposed in different systems [22–27]. These schemes took advantage of the idea of quantum interrogation, and they were local quantum gates. Although qubits in the gates did not interact with each other, they needed direct contact or indirect contact by an intermediate system between them, that is, these interaction-free quantum gates also required to transmit particles between qubits.

Here, we will demonstrate that distributed quantum computation can be achieved without transmitting any particles. A CPHASE gate between two nonlocal qubits will be constructed in the quantum-dot (QD)-microcavity coupled system, which is a promising physical system for solid-state-based quantum information processing due to the recent developments in semiconductor nanoelectronics technology. Many efforts have been made on the QD-based quantum information, such as fast initialization [28], nondestructive measurement [29], and coherent manipulation [30,31] of single-electron spins in QDs. Especially, Bonato *et al.* [32] showed that, in the weak-coupling cavity QED regime, a good interaction existed

*szhang@ybu.edu.cn

between a photon and a charged self-assembled GaAs/InAs QD. Based on the spin-selective photon reflection from a double-sided microcavity, a series of quantum information processing schemes based on the QD-microcavity system were proposed in recent years [33–37]. All the above works demonstrated that the quantum-dot system is one of the most promising candidates for the storage and manipulation of quantum information. In this paper, we propose a counterfactual distributed CPHASE gate for quantum-dot spin qubits in double-sided optical microcavities. Two nonlocal QD-microcavity units are linked by a nested Michelson-type interferometer. In order to achieve the CPHASE gate, an auxiliary single photon needs to enter the interferometer, however, we will show that the photon never passes through the channel between the two nonlocal units. Therefore, the CPHASE gate can be achieved counterfactually without transmitting any particles. The present scheme further exhibits the counterfactuality of quantum mechanics and maybe opens a different way for distributed quantum computation.

II. COUNTERFACTUAL DISTRIBUTED CPHASE GATE FOR TWO QUANTUM-DOT SPIN QUBITS

We first introduce the QD-microcavity unit. Consider a system consisting of a singly charged self-assembled GaAs/InAs QD with four relevant electronic levels, $|\uparrow\rangle$, $|\downarrow\rangle$, $|\uparrow\downarrow\Uparrow\rangle$, and $|\uparrow\downarrow\Downarrow\rangle$ as shown in Fig. 1, being embedded in an optical resonant double-sided microcavity. The charged exciton X^-, produced by the optical excitation of the system, consists of two electrons bound in one hole. The two electrons in the exciton are in a singlet state and have total spin zero, so the electron-spin interactions with the heavy-hole spin are avoided. The spin of the excess electron in the QD interacts with two types of incident circular polarization photon, one involving the photon with spin $s_z = +1$ ($|R^\uparrow\rangle$ or $|L^\downarrow\rangle$) and the other involving the photon with spin $s_z = -1$ ($|R^\downarrow\rangle$ or $|L^\uparrow\rangle$). According to the optical selection rules and the transmission and reflection rules of the cavity for an incident circular polarization photon, the interactions between photons and electrons in the QD-microcavity coupled system can be described as

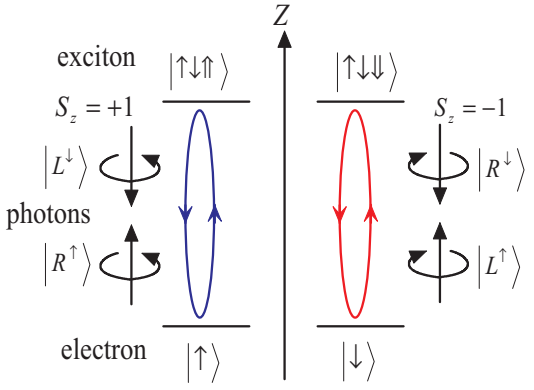

FIG. 1. (Color online) Relevant energy levels and optical selection rules for the optical transition of negatively charged exciton X^-. The superscript arrows of the photon states indicate their propagation direction along or against the z axis.

follows [32]:

$$\begin{aligned}
&|R^\uparrow,\uparrow\rangle \to |L^\downarrow,\uparrow\rangle, |L^\uparrow,\uparrow\rangle \to -|L^\uparrow,\uparrow\rangle,\\
&|R^\downarrow,\uparrow\rangle \to -|R^\downarrow,\uparrow\rangle, |L^\downarrow,\uparrow\rangle \to |R^\uparrow,\uparrow\rangle,\\
&|R^\uparrow,\downarrow\rangle \to -|R^\uparrow,\downarrow\rangle, |L^\uparrow,\downarrow\rangle \to |R^\downarrow,\downarrow\rangle,\\
&|R^\downarrow,\downarrow\rangle \to |L^\uparrow,\downarrow\rangle, |L^\downarrow,\downarrow\rangle \to -|L^\downarrow,\downarrow\rangle,
\end{aligned} \tag{1}$$

where $|R\rangle$ and $|L\rangle$ denote the right-circularly polarized photon state and the left-circularly polarized photon state, respectively, and the superscript up arrow (down arrow) denotes the propagating direction of polarized photon along (against) the z axis.

We now discuss how to counterfactually implement the CPHASE gate of two nonlocal spin qubits. The setup is shown in Fig. 2, where switchable mirrors (SMs) can be switched on and off by external means, and M_i ($i = 1,2,3,4,5$) is a normal mirror. The grey part in Alice's site and the device in Bob's site together form a Michelson-type interferometer, which, as an inner interferometer, is inserted in one of the arms of the outer Michelson interferometer formed by the light blue part and Bob's device. That is, the two optical paths $SM_1 \to M_1$ and $SM_1 \to M_3$ form the outer Michelson-type interferometer, and the two optical paths $SM_2 \to M_2$ and $SM_2 \to M_3$ form the inner Michelson-type interferometer. Optical delay ($OD_{1(2)}$) is used to match the optical path lengthes of the different paths of the interferometer. Two spin qubits belong to Alice and Bob respectively. Bob's QD-microcavity unit is inserted in one of the arms of the interferometer. Suppose the electron spins 1 and 2 are initially in the states $\alpha|\uparrow\rangle_1 + \beta|\downarrow\rangle_1$ and $\gamma|\uparrow\rangle_2 + \delta|\downarrow\rangle_2$, respectively, and the input photon is in the right circular polarization state $|R\rangle$, i.e., the initial state of the system is

$$|\psi\rangle_0 = |R\rangle(\alpha|\uparrow\rangle_1 + \beta|\downarrow\rangle_1)(\gamma|\uparrow\rangle_2 + \delta|\downarrow\rangle_2). \tag{2}$$

The photon $|R\rangle$ first enters the nested Michelson-type interferometer via the optical circulator C_1. The SM_1 is initially switched off, i.e., allowing the photon to be transmitted, but it remains on (reflects the photon) as the photon subsequently travels M cycles in the outer interferometer. After entering the interferometer, the photon is rotated an angle ϑ ($\vartheta = \pi/2M$) by the switchable polarization rotator SPR_1, i.e., $|L\rangle \to \cos\vartheta|L\rangle + \sin\vartheta|R\rangle$ and $|R\rangle \to \cos\vartheta|R\rangle - \sin\vartheta|L\rangle$. The system state becomes

$$\begin{aligned}
|\psi\rangle_0 \to\ &(\cos\vartheta|R\rangle - \sin\vartheta|L\rangle)(\alpha|\uparrow\rangle_1\\
&+ \beta|\downarrow\rangle_1)(\gamma|\uparrow\rangle_2 + \delta|\downarrow\rangle_2).
\end{aligned} \tag{3}$$

Then the photon passes through a polarizing beam splitter in the circular basis (c-PBS), which transmits the right-circularly polarized photon and reflects the left-circularly polarized photon. Thus, the $|R\rangle$ component of the photon will be propagated to the normal mirror M_1 and stays in Alice's site, and the $|L\rangle$ component of the photon will enter the inner Michelson-type interferometer via SM_2 and may be propagated to Bob's site and interact with the QD spin 1. Similar to SM_1, SM_2 is switched off initially (transmits photons) and then remains on (reflects the photon) once the photon enters into the interferometer until the photon finishes the Nth cycle in the inner interferometer.

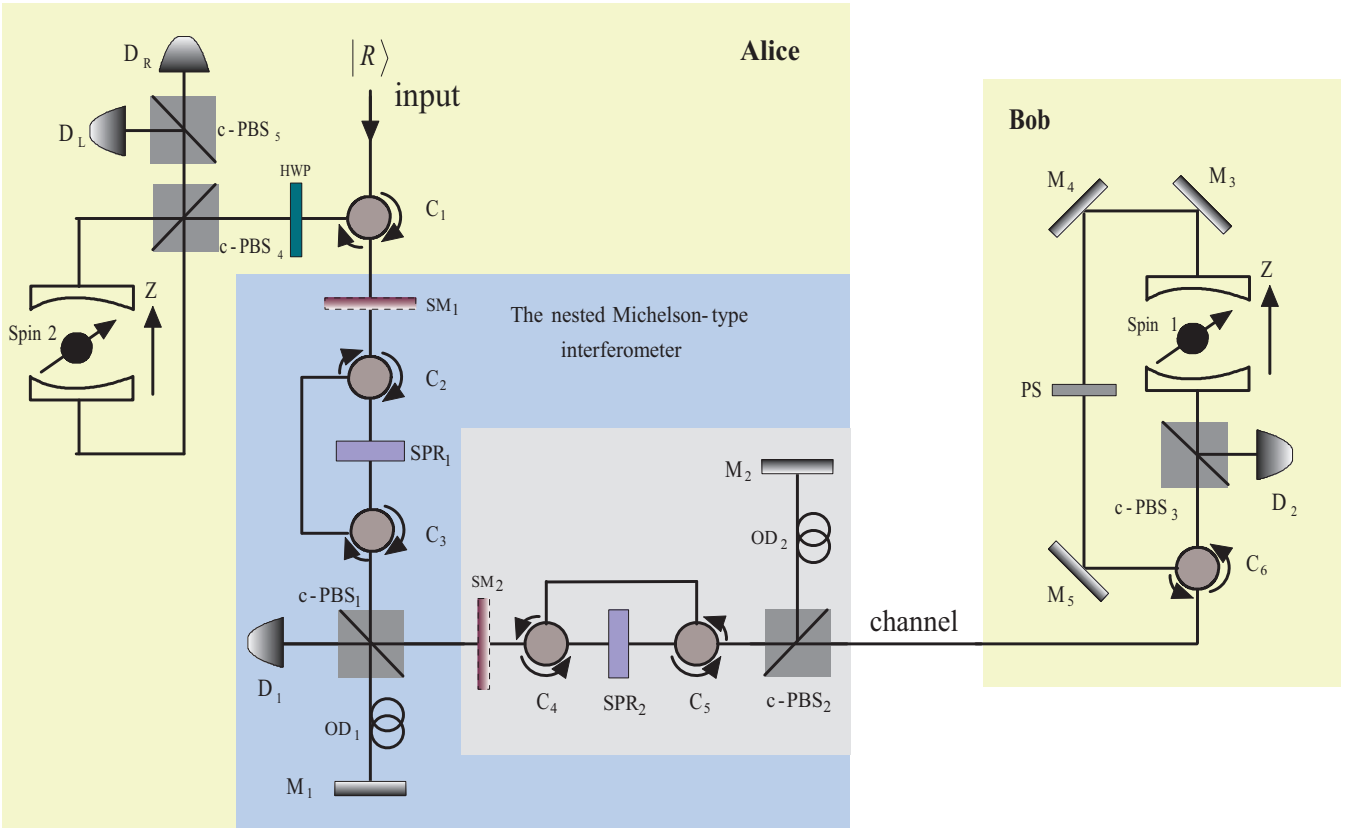

FIG. 2. (Color online) Schematic of counterfactual distributed CPHASE gate for two spin qubits. Spin 1(2) denotes the QD spin coupled with two optical microcavity. C_k and M_k ($k = 1,2,3\ldots$) are optical circulator and normal mirror, respectively. $\mathrm{SM}_{1(2)}$: switchable mirror. $\mathrm{SPR}_{1(2)}$: switchable polarization rotator, which rotates the polarization by an angle $\vartheta(\theta)$. c-PBS_k ($k = 1,2,3\ldots$): polarizing beam splitter in the circular basis. D_k ($k = 1,2,R,L$): conventional photon detector. PS is the phase shifter used to perform the transformation $|R\rangle \leftrightarrow -|R\rangle$.

Obviously, the inner interferometer is only used to achieve the interaction between the $|L\rangle$ component of the photon and the spin qubit 1 at Bob's site, so we can introduce the action of the inner interferometer using the component $|\phi\rangle \equiv |L\rangle(\alpha|\uparrow\rangle_1 + \beta|\downarrow\rangle_1)$ in Eq. (3). After passing through SM_2, the component $|L\rangle$ is first rotated as $\cos\theta|L\rangle + \sin\theta|R\rangle$ by SPR_2, that is

$$|\phi\rangle \rightarrow \cos\theta|L\rangle(\alpha|\uparrow\rangle_1 + \beta|\downarrow\rangle_1) + \sin\theta|R^{\uparrow}\rangle(\alpha|\uparrow\rangle_1 + \beta|\downarrow\rangle_1), \quad (4)$$

where $|R^{\uparrow}\rangle$ indicates the right-circular polarization will be injected into the microcavity along the z axis of the QD spin 1 by passing through c-PBS_2, C_6, and c-PBS_3 in sequence, and the component $|L\rangle$ will be reflected by c-PBS_2 and propagated to M_2. According to Eq. (1), after the photon-spin interaction, Eq. (4) will become

$$|\phi\rangle \rightarrow \cos\theta|L\rangle(\alpha|\uparrow\rangle_1 + \beta|\downarrow\rangle_1) + \alpha\sin\theta|L^{\downarrow}\rangle|\uparrow\rangle_1 - \beta\sin\theta|R^{\uparrow}\rangle|\downarrow\rangle_1. \quad (5)$$

According to Fig. 2, the $|L^{\downarrow}\rangle$ component in Bob's site will be reflected by c-PBS_3 and absorbed by the detector D_2, but the $|R\rangle$ component will undergo a π phase shift ($|R\rangle \rightarrow -|R\rangle$) from the phase shifter (PS) and come back to the SM_2 in Alice's site. Thus, for the case that the photon finishes the first cycle in the inner interferometer and the detector D_2 does not click, the state above is given by

$$|\phi\rangle \rightarrow \alpha\cos\theta|L\rangle|\uparrow\rangle_1 + (\cos\theta|L\rangle + \sin\theta|R\rangle)\beta|\downarrow\rangle_1. \quad (6)$$

Compared with Eq. (5), Eq. (6) has ignored the component $\alpha\sin\theta|L^{\downarrow}\rangle|\uparrow\rangle_1$, because the $|L^{\downarrow}\rangle$ component would be absorbed by D_2 in Bob's site. By the same process, after N inner cycles, the SM_2 is switched off to allow the photon to leave the inner interferometer, and Eq. (6) becomes

$$|\phi\rangle \rightarrow \alpha\cos^N\theta|L\rangle|\uparrow\rangle_1 + [\cos(N\theta)|L\rangle + \sin(N\theta)|R\rangle]\beta|\downarrow\rangle_1. \quad (7)$$

Therefore, by setting $\theta = \pi/2N$, the action of the N inner cycles in the inner interferometer can be represented as

$$|L\rangle(\alpha|\uparrow\rangle_1 + \beta|\downarrow\rangle_1) \rightarrow \alpha\cos^N\frac{\pi}{2N}|L\rangle|\uparrow\rangle_1 + \beta|R\rangle|\downarrow\rangle_1. \quad (8)$$

It is not difficult to calculate that the probability that D_2 does not click during the N inner cycles is $|\alpha|^2\cos^{2N}(\pi/2N) + |\beta|^2$. Now, substituting Eq. (8) into Eq. (3), the system state becomes

$$|\psi\rangle_0 \rightarrow \left[\cos\vartheta|R\rangle(\alpha|\uparrow\rangle_1 + \beta|\downarrow\rangle_1) - \sin\vartheta\left(\alpha\cos^N\frac{\pi}{2N}|L\rangle|\uparrow\rangle_1 + \beta|R\rangle|\downarrow\rangle_1\right)\right] \times (\gamma|\uparrow\rangle_2 + \delta|\downarrow\rangle_2). \quad (9)$$

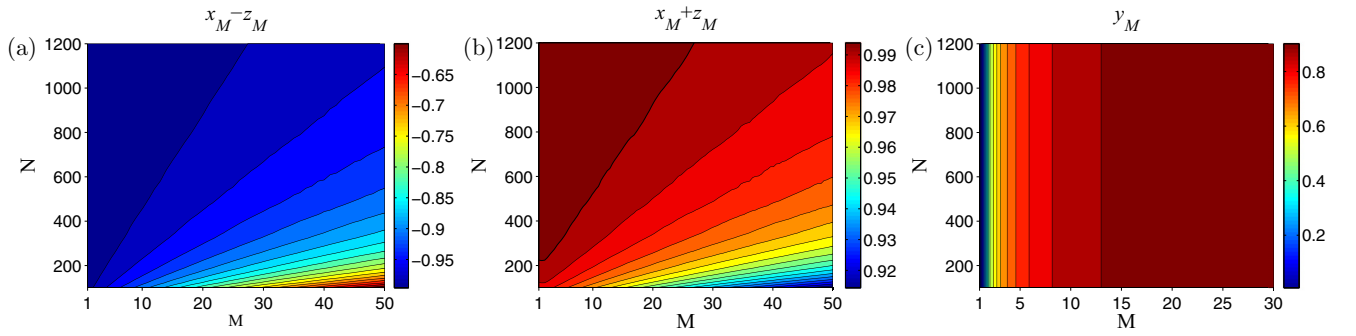

FIG. 3. (Color online) The parameters $x_M - z_M$, $x_M + z_M$, and y_M in Eq. (15) vs the different values of N and M. (a) $x_M - z_M$ is close to -1 for large N and appropriate M. (b) $x_M + z_M$ approaches 1 for appropriate values of N and M. (c) y_M is close to 1 with the increase of M and does not change with N.

Then the photon returns to c-PBS$_1$ from the inner interferometer and M_1, so the $|R\rangle$ component coming from the inner interferometer will be transmitted by c-PBS$_1$ and absorbed by the detector D_1, and other components will return to SM$_1$. Now the first outer cycle is finished, and the joint system state evolves to

$$|\psi\rangle_1 = \Big[\cos\vartheta|R\rangle(\alpha|\uparrow\rangle_1 + \beta|\downarrow\rangle_1) - \alpha\sin\vartheta\cos^N\frac{\pi}{2N}|L\rangle|\uparrow\rangle_1\Big](\gamma|\uparrow\rangle_2 + \delta|\downarrow\rangle_2). \quad (10)$$

Repeat the process from Eq. (2) to Eq. (10) M times, i.e., the photon finishes M outer cycles, the system state can be written as

$$|\psi\rangle_M = [\alpha x_M|R\rangle|\uparrow\rangle_1 + \beta y_M|R\rangle|\downarrow\rangle_1 - \alpha z_M|L\rangle|\uparrow\rangle_1] \times(\gamma|\uparrow\rangle_2 + \delta|\downarrow\rangle_2), \quad (11)$$

where the parameters x_M, y_M, and z_M satisfy the recursion relations

$$\begin{aligned} x_M &= x_{M-1}\cos\vartheta - z_{M-1}\sin\vartheta, \\ y_M &= y_{M-1}\cos\vartheta, \\ z_M &= (x_{M-1}\sin\vartheta + z_{M-1}\cos\vartheta)\cos^N\frac{\pi}{2N}, \end{aligned} \quad (12)$$

with $x_1 = y_1 = \cos\vartheta$ and $z_1 = \sin\vartheta\cos^N(\pi/2N)$. Then SM$_1$ is switched off and the photon leaves the outer interferometer. Next, the photon is rotated by a half-wave plate (HWP) oriented at 22.5° [$|R\rangle \to (1/\sqrt{2})(|R\rangle + |L\rangle)$, $|L\rangle \to (1/\sqrt{2})(|R\rangle - |L\rangle)$]. After passing through c-PBS$_4$, the component $|R\rangle$ ($|L\rangle$) will be injected into the microcavity against (along) the z axis of the QD spin 2. Hence the system state can be expressed as

$$|\psi\rangle_M \to \frac{1}{\sqrt{2}}[\alpha x_M(|R^\downarrow\rangle + |L^\uparrow\rangle)|\uparrow\rangle_1 + \beta y_M(|R^\downarrow\rangle + |L^\uparrow\rangle)|\downarrow\rangle_1 - \alpha z_M(|R^\downarrow\rangle - |L^\uparrow\rangle)|\uparrow\rangle_1](\gamma|\uparrow\rangle_2 + \delta|\downarrow\rangle_2). \quad (13)$$

The photon enters the microcavity at Alice's site to interact with spin 2. According to Eq. (1), we can obtain

$$\begin{aligned} &(|R^\downarrow\rangle + |L^\uparrow\rangle)(\gamma|\uparrow\rangle_2 + \delta|\downarrow\rangle_2) \\ &\quad\to (|R^\downarrow\rangle + |L^\uparrow\rangle)(-\gamma|\uparrow\rangle_2 + \delta|\downarrow\rangle_2), \\ &(|R^\downarrow\rangle - |L^\uparrow\rangle)(\gamma|\uparrow\rangle_2 + \delta|\downarrow\rangle_2) \\ &\quad\to (-|R^\downarrow\rangle + |L^\uparrow\rangle)(\gamma|\uparrow\rangle_2 + \delta|\downarrow\rangle_2). \end{aligned} \quad (14)$$

By substituting Eq. (14) into Eq. (13), the resulting photon-electron state can be obtained:

$$\begin{aligned} |\psi\rangle_M \to\ & \frac{1}{\sqrt{2}}|R\rangle[-\alpha\gamma(x_M - z_M)|\uparrow\rangle_1|\uparrow\rangle_2 \\ &+ \alpha\delta(x_M + z_M)|\uparrow\rangle_1|\downarrow\rangle_2 \\ &- \beta\gamma y_M|\downarrow\rangle_1|\uparrow\rangle_2 + \beta\delta y_M|\downarrow\rangle_1|\downarrow\rangle_2] \\ &+ \frac{1}{\sqrt{2}}|L\rangle[-\alpha\gamma(x_M + z_M)|\uparrow\rangle_1|\uparrow\rangle_2 \\ &+ \alpha\delta(x_M - z_M)|\uparrow\rangle_1|\downarrow\rangle_2 \\ &- \beta\gamma y_M|\downarrow\rangle_1|\uparrow\rangle_2 + \beta\delta y_M|\downarrow\rangle_1|\downarrow\rangle_2]. \end{aligned} \quad (15)$$

We plot the variation trend of the parameters $x_M - z_M$, $x_M + z_M$, and y_M with the values of N and M, as shown in Fig. 3. It can be seen that $(x_M - z_M) \sim -1$, $(x_M + z_M) \sim 1$, and $y_M \sim 1$ for large values of N and M. Therefore, by choosing suitable outer (inner) cycle numbers M (N), which can be controlled by choosing a switching time of SM$_{1(2)}$, the final state can be approximately written as

$$\begin{aligned} |\psi\rangle_M \to\ & \frac{1}{\sqrt{2}}|R\rangle[\alpha\gamma|\uparrow\rangle_1|\uparrow\rangle_2 + \alpha\delta|\uparrow\rangle_1|\downarrow\rangle_2 \\ &- \beta\gamma|\downarrow\rangle_1|\uparrow\rangle_2 + \beta\delta|\downarrow\rangle_1|\downarrow\rangle_2] \\ &- \frac{1}{\sqrt{2}}|L\rangle[\alpha\gamma|\uparrow\rangle_1|\uparrow\rangle_2 + \alpha\delta|\uparrow\rangle_1|\downarrow\rangle_2 \\ &+ \beta\gamma|\downarrow\rangle_1|\uparrow\rangle_2 - \beta\delta|\downarrow\rangle_1|\downarrow\rangle_2]. \end{aligned} \quad (16)$$

After being either transmitted or reflected by the optical cavity, the photon is forwarded to c-PBS$_4$, c-PBS$_5$, and detectors, which are used to measure the polarization of the photon. From Eq. (16), we can see, if the photon is in the state $|L\rangle$ (D_L clicks), the CPHASE gate of two spin qubits is directly achieved; if the photon is in the state $|R\rangle$ (D_R clicks), the CPHASE gate can also be accomplished by performing a σ_Z operation on electron spin 1.

By now, the distributed CHPASE gate has been achieved by repeatedly using the nested Michelson-type interferometer. Reviewing the whole process, we can see that the incident photon has played a critical role, but it has never passed

through the transmission channel between Alice and Bob. That is because as long as the photon passed through the channel, on the way back from Bob's site to Alice's site, the components $|L\rangle$ and $|R\rangle$ would be absorbed by D_2 and D_1 respectively, and the photon cannot interact with spin 2. The scheme suppresses the probability that the photon enters the transmission channel by repeatedly using the nested Michelson-type interferometer, which ensures that the distributed CPHASE gate can be implemented without transmitting any physical particles. Therefore, compared with the existing schemes, the present one is counterfactual.

III. DISCUSSION AND CONCLUSIONS

Now we begin to analyze and discuss the performance of the present scheme in the practical experiment and some practical issues that may affect the implementation of the scheme. The key procedure of the scheme is choosing suitable values of the outer cycles M and inner cycles N, i.e., the photon's rotated angles θ and ϑ by SPR_1 and SPR_2, which can suppress the probability that the photon passes through the channel. Therefore, the value of $M(N)$ directly affects the success probability of the counterfactual scheme. From the section above, we can see that the scheme will succeed only when the photon is not absorbed by detector D_1 or D_2, so the success probability is equivalent to the probability that both detectors D_1 and D_2 did not click. We numerically evaluate the success probability change with M and N as shown in Fig. 4, which shows that the scheme can be achieved successfully for large M and N. For example, the success probability $P = 0.9169$ for $M = 20$ and $N = 500$, and $P = 0.9615$ for $M = 60$ and $N = 2000$. The cycle numbers M and N are determined by the switching time of SM_1 and SM_2, respectively. For the given optical path length and $M(N)$, the required switching time of $\mathrm{SM}_{1(2)}$ can be easily worked out. Experimentally, the $\mathrm{SM}_{1(2)}$ can be controlled accurately by a computer via the switching-time sequences [36,38,39]. What is more, ultrafast optical switches without disturbing the photon's quantum state have been demonstrated with a switching window of 10 ps [40,41].

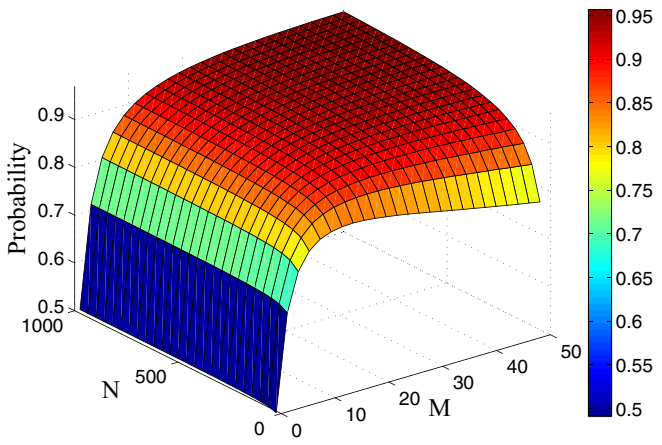

FIG. 4. (Color online) The success probability of counterfactual distributed CHPASE gate vs different values of outer and inner cycles M and N.

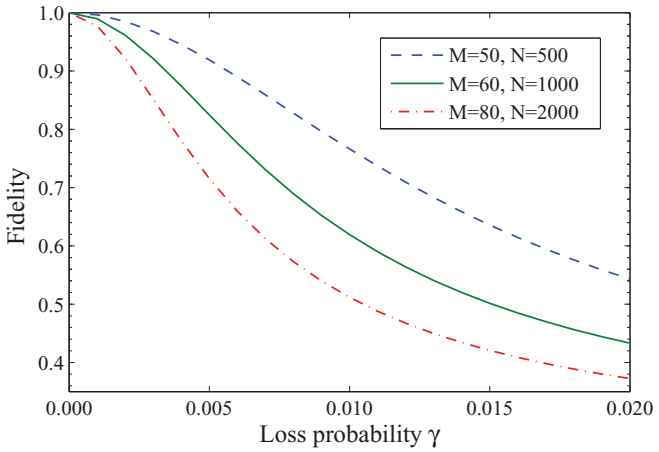

FIG. 5. (Color online) The average fidelity of the counterfactual distributed CPHASE gate vs the loss probability γ for the different values of M and N.

From the analysis above, we can see that the gate operation requires large cycle values M and N, so the photon's loss in the transmission process will be a critical influence factor for the gate performance. To quantitatively analyze the effect of loss, we can define the loss probability as γ, which indicates the probability that the photon is absorbed by other objects in the transmission channel of every cycle rather than detector D_1 or D_2. Then we rederive the process of the distributed CPHASE gate with the loss probability γ. By evaluating the fidelity of the CPHASE gate, we can qualify the influence of loss. The gate fidelity is defined as [42] $\mathcal{F} = \overline{\langle\psi_0|U^\dagger\rho_t U|\psi_0\rangle}$, where the overline indicates the average over all possible input states $|\psi_0\rangle$, U is the ideal CPHASE gate (note that here U is the CPHASE gate in the case of given values of M and N rather than the complete ideal CPHASE gate), and ρ_t is the density matrix of the final state after the practical CPHASE gate operation. We numerically evaluate the gate fidelity for different values of γ, M, and N in Fig. 5. It can be seen that the present scheme is sensitive to loss, and the CPHASE gate has higher fidelity when the loss probability is suppressed under about 0.5%. The success probability of the scheme is also affected by the loss in the similar manner. For example, it can be calculated when $\gamma = 0.2\%$, $M = 60$, and $N = 1000$, the fidelity $\mathcal{F} = 96.16\%$ and the success probability $\mathcal{P} = 73.06\%$. Therefore, the present CPHASE gate can function well with better performance for lower loss probability.

The basic module in the present scheme is the QD-microcavity system. Note that the optical transition rules in Eq. (1) were obtained without regard to the side leakage and cavity loss. When these factors are not negligible, the reflection and transmission rules of the coupled and the uncoupled cavities in Eq. (1) need to be modified. Suppose that the coupling strength between X^- and the cavity field is g; the cavity field decay rate, the side leakage rate, and the X^- dipole decay rate are described by κ, κ_s, and γ, respectively. The reflection and transmission coefficients of a double-sided optical microcavity for weak excitation limit can be described

by [33,34]

$$r(\omega)=\frac{\left[i(\omega_{X^-}-\omega)+\frac{\gamma}{2}\right]\left[i(\omega_c-\omega)+\frac{\kappa_s}{2}\right]+g^2}{\left[i(\omega_{X^-}-\omega)+\frac{\gamma}{2}\right]\left[i(\omega_c-\omega)+\kappa+\frac{\kappa_s}{2}\right]+g^2},$$
$$t(\omega)=\frac{-\kappa\left[i(\omega_{X^-}-\omega)+\frac{\gamma}{2}\right]}{\left[i(\omega_{X^-}-\omega)+\frac{\gamma}{2}\right]\left[i(\omega_c-\omega)+\kappa+\frac{\kappa_s}{2}\right]+g^2}, \quad (17)$$

where ω, ω_c, and ω_{X^-} are respectively the frequencies of the input photon, the cavity field, and the X^- transition. For the cold cavity, i.e., the QDs do not couple to the cavity field ($g=0$), under the resonant interaction condition $\omega_c=\omega_{X^-}=\omega_0$, the reflection and transmission coefficients become

$$r_0(\omega)=\frac{i(\omega_0-\omega)+\frac{\kappa_s}{2}}{i(\omega_0-\omega)+\kappa+\frac{\kappa_s}{2}},$$
$$t_0(\omega)=\frac{-\kappa}{i(\omega_c-\omega)+\kappa+\frac{\kappa_s}{2}}. \quad (18)$$

Therefore, under the realistic case of considering the side leakage and the cavity loss, the rules of optical transitions in Eq. (1) become [33,34]

$$\begin{aligned}
|R^{\uparrow},\uparrow\rangle &\rightarrow |r(\omega)||L^{\downarrow},\uparrow\rangle+|t(\omega)||R^{\uparrow},\uparrow\rangle,\\
|R^{\downarrow},\downarrow\rangle &\rightarrow |r(\omega)||L^{\uparrow},\downarrow\rangle+|t(\omega)||R^{\downarrow},\downarrow\rangle,\\
|L^{\uparrow},\downarrow\rangle &\rightarrow |r(\omega)||R^{\downarrow},\downarrow\rangle+|t(\omega)||L^{\uparrow},\downarrow\rangle,\\
|R^{\uparrow},\downarrow\rangle &\rightarrow -|t_0(\omega)||R^{\uparrow},\downarrow\rangle-|r_0(\omega)||L^{\downarrow},\downarrow\rangle,\\
|R^{\downarrow},\uparrow\rangle &\rightarrow -|t_0(\omega)||R^{\downarrow},\uparrow\rangle-|r_0(\omega)||L^{\uparrow},\uparrow\rangle,\\
|L^{\uparrow},\uparrow\rangle &\rightarrow -|t_0(\omega)||L^{\uparrow},\uparrow\rangle-|r_0(\omega)||R^{\downarrow},\uparrow\rangle.
\end{aligned} \quad (19)$$

We need to derive the realistic evolution of the system state during the process of the CPHASE gate operation by replacing the optical transitions in Eq. (1) with Eq. (19). To qualify the effect of the side leakage and the cavity loss on the performance of the CPHASE gate, it is necessary to evaluate the fidelity of the CPHASE gate by some tedious calculations. We numerically simulate the varying of the fidelity of the final photon-spin state versus κ_s/κ and g/κ for $N=500$ and $M=60$ as shown in Fig. 6, which shows that the cavity side leakage and cavity field decay have an obvious effect on the gate fidelity, and the effect from κ_s/κ is greater than g/κ. The scheme has higher fidelity for $\kappa_s \ll \kappa$, for example $\mathcal{F}=95.13\%$ for $\kappa_s=0.1\kappa$ and $g=3\kappa$, and $\mathcal{F}=98.19\%$ for $\kappa_s=0.01\kappa$ and $g=0.5\kappa$. The present scheme requires a microcavity with lower side leakage, which can be suppressed with the improvement of fabrication techniques [43]. The weak coupling with $g<(\kappa+\kappa_s+\gamma)/4$ can be easily achieved in experiment, and the electron spin qubit used in the present scheme and its fast initialization have also been demonstrated [21,28].

The electron-spin decoherence will also reduce the fidelity of the scheme. In the GaAs/InAs QD, the decoherence of the excess electron spin is mainly caused by the hyperfine interaction between the electron and the nuclear spins. Describe the electron-spin relaxation time and coherence time by T_1^e and T_2^e. Generally, T_1^e is considerably larger than T_2^e [44], which means that the fidelity of the scheme is affected by pure-dephasing processes on the time scale T_2^e and the effective gate operation should be achieved in the time T_2^e. The spin decoherence will decrease the fidelity by a factor

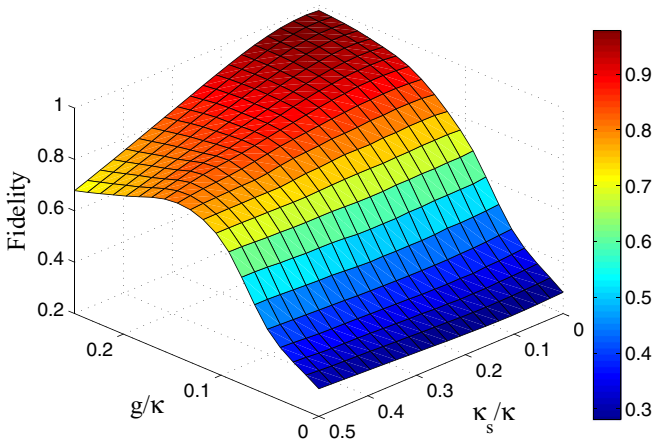

FIG. 6. (Color online) The fidelity of counterfactual distributed CHPASE gate for the case $N=500$ and $M=60$ vs the side leakage rate κ_s/κ and the normalized coupling strength g/κ. Here we have set $\gamma=0.1\kappa$, which is experimentally achievable.

$F'=[1+\exp(-\Delta t/T_2^e)]/2$ [33,34], where Δt is the time interval between two inputs of a photon. In the present scheme, only when the photon completed the M outer cycles, it can enter into the cavity 2, so the Δt here is actually the time from the release of the photon until it is measured. The scheme requires the photon to travel many cycles in the interferometer, and the CPHASE gate should be completed within the electron-spin coherence time, i.e., $\Delta t < T_2^e$. Therefore, the coherence time not only affects the fidelity but also limits the distance between the two nodes. The approach to prolonging the electron-spin coherence time is to suppress nuclear spin fluctuations. In recent years, many works have demonstrated that spin-echo techniques can greatly suppress the nuclear spin fluctuations effectively and prolong the electron spin coherence [44–48]. Especially, recent experiment has showed dephasing time T_2^e can exceed hundreds of microseconds by using spin-echo techniques and a multiple-pulse Carr-Purcell-Meiboom-Gill echo sequence [49,50]. In the present scheme, we suppose the optical path length between the two QD-cavity units is L, so the required time to achieve the counterfactual CPHASE gate is $\Delta t \approx 2NML/c$ (c is the speed of light). For the coherent time $T_2^e \sim 200\ \mu$s, $\Delta t \sim 100\ \mu$s, $M=30$, and $N=500$, we can obtain the fidelity $F'=0.8033$ and the distance between the two nodes is limited to the scale of meter magnitude.

In addition, the detectors D_1 and D_2 in the present scheme are only used to absorb the photon passed through the transmission channels, so the sensitivity and dark counts of the detectors does not influence the efficiency of the scheme. Hence these detectors can even be replaced with other absorption objects. While the detection efficiency of D_R and D_L will affect the performance of the CPHASE gate, that is because the successful achievement of the scheme is dependent on the detection results of $D_{R(L)}$. Nevertheless, D_R and D_L are only required to distinguish the vacuum and nonvacuum state rather than distinguish the number of the photons, which thus decreases the requirements of the photon detection in practical realization.

Note that the key component in the present scheme is the quantum-dot-microcavity unit, which can control the

transmission or absorption of right-circularly polarized photons by the quantum state of the electron spin. In this sense, as long as the quantum control device can be achieved, the present scheme is universal for other systems. Some alternative quantum control devices have also been proposed in previous quantum zeno style gates [22–27]. These local quantum gates were essentially achieved by use of the quantum version of interaction-free measurement, so they needed to exchange particles between two quantum nodes. In principle, these schemes can be straightway extended to the counterfactual distributed quantum gates without transmitting any particles as proposed here, however, this extension might be unpractical because of their complicated circuits and intrinsic difficulties of their physical systems. For example, Ref. [22] proposed that interaction-free quantum computation can be achieved using flying electrons and positrons, and the implementation of this scheme needed to employ an accelerator, which no doubt increased experimental difficulty and cost. The schemes with single-atom and single-photon qubits required strong coupling between photon and atom [24–26], otherwise the probability of success is very small. For this reason, Ref. [27] suggested that the Rydberg atom ensemble can be used to construct photon gates. The proposal used the photon's dual-rail path encoding and used the combined system of single atom and atom ensemble as the intermediate system, which also increased the complexity of the experimental implementation. Therefore, by contrast, maybe the present scheme is more realistic.

In conclusion, we have proposed a counterfactual scheme for a distributed CPHASE gate between two distant quantum-dot electron-spin qubits in optical microcavities. Compared with the existing distributed quantum computation schemes, the present scheme does not need to transmit any particles between two distant nodes in the quantum network. The results of numerical analysis on the effect of experimental imperfections showed that the scheme can be effectively implemented with high fidelity in the ideal asymptotic limit. Once the distributed CPHASE gates are implemented, the distributed universal quantum computation and nonlocal entanglement generation can be straightway achieved. Though the present scheme requires high experimental conditions, perhaps the fact that two spatially separated qubits can be controlled by each other without transmitting any particles is more interesting, and the fundamental idea may be useful.

ACKNOWLEDGMENTS

This work was supported by the National Natural Science Foundation of China under Grants No. 61465013, No. 11465020, and No. 11264042; the Program for Chun Miao Excellent Talents of Jilin Provincial Department of Education under Grant No. 201316; and the Talent Program of Yanbian University of China under Grant No. 950010001.

[1] A. C. Elitzur and L. Vaidman, Found. Phys. **23**, 987 (1993).
[2] P. Kwiat, H. Weinfurter, T. Herzog, A. Zeilinger, and M. A. Kasevich, Phys. Rev. Lett. **74**, 4763 (1995).
[3] O. Hosten, M. T. Rakher, J. T. Barreiro, N. A. Peters, and P. G. Kwiat, Nature (London) **439**, 949 (2006).
[4] T.-G. Noh, Phys. Rev. Lett. **103**, 230501 (2009).
[5] Y. Liu, L. Ju, X.-L. Liang, S.-B. Tang, G.-L. S. Tu, L. Zhou, C.-Z. Peng, K. Chen, T.-Y. Chen, Z.-B. Chen, and J.-W. Pan, Phys. Rev. Lett. **109**, 030501 (2012).
[6] G. Brida, A. Cavanna, I. P. Degiovanni, M. Genovese, and P. Traina, Laser Phys. Lett. **9**, 247 (2012).
[7] Z. Q. Yin, H. W. Li, W. Chen, Z. F. Han, and G. C. Guo, Phys. Rev. A **82**, 042335 (2010).
[8] Z. Q. Yin, H. W. Li, Y. Yao, C. M. Zhang, S. Wang, W. Chen, G. C. Guo, and Z. F. Han, Phys. Rev. A **86**, 022313 (2012).
[9] H. Salih, Z. H. Li, M. Al-Amri, and M. S. Zubairy, Phys. Rev. Lett. **110**, 170502 (2013).
[10] N. Gisin, Phys. Rev. A **88**, 030301 (2013).
[11] J. L. Zhang, F. Z. Guo, F. Gao, B. Liu, and Q. Y. Wen, Phys. Rev. A **88**, 022334 (2013).
[12] Q. Guo, L. Y. Cheng, L. Chen, H. F. Wang, and S. Zhang, Opt. Express **22**, 8970 (2014).
[13] M. A. Nielsen and I. L. Chuang, *Quantum Computation and Quantum Information* (Cambridge University Press, Cambridge, England, 2000).
[14] L. K. Grover, arXiv:quant-ph/9607024.
[15] J. I. Cirac, A. K. Ekert, S. F. Huelga, and C. Macchiavello, Phys. Rev. A **59**, 4249 (1999).
[16] Y. L. Lim, A. Beige, and L. C. Kwek, Phys. Rev. Lett. **95**, 030505 (2005).
[17] Y. F. Xiao, X. M. Lin, J. Gao, Y. Yang, Z. F. Han, and G. C. Guo, Phys. Rev. A **70**, 042314 (2004).
[18] X. F. Zhou, Y. S. Zhang, and G. C. Guo, Phys. Rev. A **71**, 064302 (2005).
[19] A. Serafini, S. Mancini, and S. Bose, Phys. Rev. Lett. **96**, 010503 (2006).
[20] L. Jiang, J. M. Taylor, A. S. Sørensen, and M. D. Lukin, Phys. Rev. A **76**, 062323 (2007).
[21] X. Q. Shao, H. F. Wang, L. Chen, S. Zhang, Y. F. Zhao, and K. H. Yeon, J. Opt. Soc. Am. B **26**, 2440 (2009).
[22] H. Azuma, Phys. Rev. A **70**, 012318 (2004).
[23] J. D. Franson, B. C. Jacobs, and T. B. Pittman, Phys. Rev. A **70**, 062302 (2004).
[24] A. A. Methot and K. Wicker, arXiv:quant-ph/0109105.
[25] Y. P. Huang and M. G. Moore, Phys. Rev. A **77**, 062332 (2008).
[26] M. Pavičić, Phys. Rev. A **75**, 032342 (2007).
[27] J. C. Garcia-Escartin and P. Chamorro-Posada, Phys. Rev. A **85**, 032309 (2012).
[28] C. Emary, X. Xu, D. G. Steel, S. Saikin, and L. J. Sham, Phys. Rev. Lett. **98**, 047401 (2007).
[29] D. Kim, S. E. Economou, S. C. Badescu, M. Scheibner, A. S. Bracker, M. Bashkansky, T. L. Reinecke, and D. Gammon, Phys. Rev. Lett. **101**, 236804 (2008).
[30] D. Press, T. D. Ladd, B. Zhang, and Y. Yamamoto, Nature (London) **456**, 218 (2008).

[31] E. D. Kim, K. Truex, X. Xu, B. Sun, D. G. Steel, A. S. Bracker, D. Gammon, and L. J. Sham, Phys. Rev. Lett. **104**, 167401 (2010).
[32] C. Bonato, F. Haupt, S. S. R. Oemrawsingh, J. Gudat, D. Ding, M. P. van Exter, and D. Bouwmeester, Phys. Rev. Lett. **104**, 160503 (2010).
[33] C. Y. Hu, W. J. Munro, J. L. O'Brien, and J. G. Rarity, Phys. Rev. B **80**, 205326 (2009).
[34] C. Y. Hu and J. G. Rarity, Phys. Rev. B **83**, 115303 (2011).
[35] T. J. Wang, S. Y. Song, and G. L. Long, Phys. Rev. A **85**, 062311 (2012).
[36] H. R. Wei and F. G. Deng, Phys. Rev. A **87**, 022305 (2013).
[37] H. F. Wang, A. D. Zhu, S. Zhang, and K. H. Yeon, Phys. Rev. A **87**, 062337 (2013).
[38] Q. Chen and M. Feng, Phys. Rev. A **79**, 064304 (2009).
[39] Q. Chen and M. Feng, Phys. Rev. A **82**, 052329 (2010).
[40] M. A. Hall, J. B. Altepeter, and P. Kumar, Phys. Rev. Lett. **106**, 053901 (2011).
[41] P. C. Humphreys, B. J. Metcalf, J. B. Spring, M. Moore, X. M. Jin, M. Barbieri, W. S. Kolthammer, and I. A. Walmsley, Phys. Rev. Lett. **111**, 150501 (2013).
[42] J. F. Poyatos, J. I. Cirac, and P. Zoller, Phys. Rev. Lett. **78**, 390 (1997).
[43] S. Reitzenstein, C. Hofmann, A. Gorbunov, M. Strauß, S. H. Kwon, C. Schneider, A. Löffler, S. Höfling, M. Kamp, and A. Forchel, Appl. Phys. Lett. **90**, 251109 (2007).
[44] A. Pineiro-Orioli, D. P. S. McCutcheon, and T. Rudolph, Phys. Rev. B **88**, 035315 (2013).
[45] J. R. Petta, A. C. Johnson, J. M. Taylor, E. A. Laird, A. Yacoby, M. D. Lukin, C. M. Marcus, M. P. Hanson, and A. C. Gossard, Science **309**, 2180 (2005).
[46] F. H. L. Koppens, K. C. Nowack, and L. M. K. Vandersypen, Phys. Rev. Lett. **100**, 236802 (2008).
[47] S. M. Clark, K.-M. C. Fu, Q. Zhang, T. D. Ladd, C. Stanley, and Y. Yamamoto, Phys. Rev. Lett. **102**, 247601 (2009).
[48] D. Press, K. De Greve, P. L. McMahon, T. D. Ladd, B. Friess, C. Schneider, M. Kamp, S. Höfling, A. Forchel, and Y. Yamamoto, Nat. Photon. **4**, 367 (2010).
[49] H. Bluhm, S. Foletti, I. Neder, M. Rudner, D. Mahalu, V. Umansky, and A. Yacoby, Nat. Phys. **7**, 109 (2011).
[50] Z. L. Xiang, S. Ashhab, J. Q. You, and F. Nori, Rev. Mod. Phys. **85**, 623 (2013).